*Article citation info:*
Marimuthu K, Sundararaj AJ, Nair AG, Muthumari T. Experimental and kinetic analysis of low to intermediate temperature auto-ignition of binary ethylene-acetylene blends. Combustion Engines. 0000;XXX(X):xx-xx. https://doi.org/10.19206/CE-217944

*Kesavan MARIMUTHU*
*Aldin Justin SUNDARARAJ*
*Abhijith Girish NAIR*
*Thangapandi MUTHUMARI*

**Combustion Engines**
Polish Scientific Society of Combustion Engines

# Experimental and kinetic analysis of low to intermediate temperature auto-ignition of binary ethylene-acetylene blends

ARTICLE INFO

Received: 25 January 2026
Revised: 6 February 2026
Accepted: 9 February 2026
Available online: 13 February 2026

*Understanding the ignition characteristics of binary hydrocarbon blends is essential for designing high-speed propulsion systems such as scramjets, where ignition under short residence time is a critical challenge. In this work, the ignition delay behaviour of ethylene-acetylene/air mixtures was examined through shock tube experiments and kinetic simulations under engine-relevant conditions. Ethylene was used as the primary fuel and blended with acetylene at 5%, 10%, and 20% by volume to form binary mixtures, at an equivalence ratio of 1.0, temperatures between 560–1030 K, and pressures of 2.5–9 bar. The ignition delay time was determined from peak pressure rise and CH* chemiluminescence behind the reflected shock. Unlike previous blended fuel studies dominated by saturated hydrocarbons, this work presents a comprehensive dataset for ethylene-acetylene blends at low to intermediate temperatures and increasing the acetylene fraction from 5% to 20% reduces the ignition delay time by up to 50–60% in the 700–850 K and 2–5 bar regime. Numerical simulations were performed using ANSYS Chemkin in a closed, homogeneous, constant-volume reactor with the NUIG, ARAMCO, LLNL, and San Diego mechanisms. The sensitivity and rate-of-production analyses reveal that ignition is governed by $HO_2$–$H_2O_2$ radical chemistry, with the thermal decomposition of $H_2O_2$ triggering rapid OH formation. Acetylene enhances ignition by promoting the regeneration of HCCO radicals and accelerating the transition to chain-branching chemistry.*

Key words: *auto ignition, chemical kinetics, fuel blends, sensitivity and rate-of-production analysis*



## 1. Introduction

The development of combustion models for high-speed propulsion systems requires a comprehensive understanding of the ignition characteristics of unsaturated hydrocarbons, alongside a detailed knowledge of the fundamental chemical kinetics governing the oxidation pathways of small hydrocarbon intermediates. Ethylene ($C_2H_4$) and acetylene ($C_2H_2$) are within the lower hydrocarbon combustion chemistry. These compounds are widespread products originating from the pyrolysis and oxidation of nearly all larger alkanes and alkenes, and their subsequent consumption significantly alters global reaction kinetics, characteristics of flame propagation, and the formation pathways of pollutants, including the elaborate chemistry that leads to soot precursors. Ethylene acts as a critical transitional entity in the degradation of higher hydrocarbons, facilitating the reactivity transition between saturated and unsaturated compounds. In contrast, acetylene, distinguished by its strong triple bond and heightened chemical reactivity, functions as both a catalyst for chain branching and an essential precursor for soot and polycyclic aromatic hydrocarbons. The chemical interaction between these two species profoundly affects ignition characteristics, flame dynamics, and emissions within hydrocarbon combustion systems. Experimental data on the ignition behaviour of binary ethylene-acetylene mixtures are limited, restricting the validation of detailed kinetic mechanisms. Ignition delay time, defined as the interval between the arrival of the reflected shock and ignition onset, provides a direct measure of fuel reactivity. Recent studies have shown that ignition delay measurements strongly depend on the start of combustion, particularly at low and intermediate temperatures where pressure rise is weak. Boruc et al. [3] established that optical diagnostics, such as radical chemiluminescence, provide more reliable and repeatable ignition delay measurements than pressure-based methods alone, especially for fuels with long induction periods. Shock tube experiments enable reliable IDT measurements under well-controlled, near-constant-volume conditions across wide temperature and pressure ranges. These measurements provide the foundation for validating detailed chemical kinetic mechanisms that support computational modelling frameworks such as CHEMKIN. Such validation is particularly essential within the low-to-intermediate temperature range, where the majority of kinetic models continue to demonstrate substantial uncertainties in accurately capturing the oxidation behaviour of $C_2$–$C_3$ unsaturated hydrocarbons [11]. Several shock-tube and rapid-compression-machine investigations have measured ignition delay times for individual $C_2$–$C_3$ hydrocarbons across wide pressure and temperature ranges, forming the core validation datasets for kinetic mechanisms such as NUIG and Aramco Mechanism. The current study aims to address the lack of IDT data for binary $C_2H_4/C_2H_2$ blends, quantify the effect of acetylene addition, and identify dominant radical pathways over a wide range of low-intermediate temperatures.

Earlier studies on pure ethylene, ethane, and propane have consistently highlighted the fundamental kinetic features governing their oxidation behaviour. Across a broad range of pressures (1–40 bar) and temperatures (700–2600 K), extensive experimental datasets have mapped ignition delay characteristics, chain-branching pathways, and temperature-regime transitions for these $C_2$–$C_3$ hydrocarbons [8, 17, 24, 32]. Foundational shock tube investigations by Burcat & Lifshitz [4], de Vries [8], and Kopp [16] established the high-temperature ignition delay behaviour of

ethylene and ethane, including the sensitivity to equivalence ratio, dilution, and pressure. Propane oxidation has similarly been characterised through both shock tube and rapid compression machine (RCM) measurements, with Gallagher et al. [10] providing key high-pressure ignition data. Dagaut and co-workers [6, 7] performed detailed speciation studies in JSRs for ethylene, ethane, and propane at pressures up to 10 bar (800–1250 K) and validated the hierarchical development of chemical mechanisms, which build $C_1$–$C_2$ core sub-mechanisms upward to larger fuels. High-pressure, intermediate-temperature datasets continue to reveal important kinetic gaps. Herzler [11] reported propane-air ignition delays at 10–30 bar and 900–1300 K, identifying a pronounced drop in apparent activation energy below 1050 K and demonstrating that multiple detailed mechanisms systematically overpredict ignition delays in this region, demonstrating strong low-temperature chain-branching driven by propyl-peroxy isomerisation pathways. Complementary shock-tube work by Walker [31] on $CH_4$/$C_2H_6$ mixtures (1180–2248 K, 1 atm) confirmed that modest ethane additions strongly shorten ignition delays, with the largest incremental effect at low ethane fractions, while revealing increasing model experiment divergence as ethane concentration rises. Shock-tube investigations by De Vries & Petersen [9] performed a systematic shock-tube study of methane-based binary and ternary blends (L21 design) at gas-turbine-relevant conditions (20 atm, 800 K, $\phi$ = 0.5) and they report a mean ignition time near 7.9 ms ($\sigma \approx$ 1.9 ms) for the tested blends and document a pronounced low-temperature (NTC-like) reduction in apparent activation energy that causes ignition to be much faster than extrapolation from high-temperature data would predict, where existing mechanisms fail to capture. Engine-based studies have further confirmed that modifying fuel composition directly affects autoignition delay and combustion phasing, strengthening the broader relevance of ignition delay studies for practical propulsion and energy systems [23]. Early work by Holton et al. [12] measured autoignition delay times in an atmospheric flow reactor for methane, ethane, propane and representative binary/ternary methane-based blends across 930–1140 K and equivalence ratios 0.5–1.25, and measured delays for premixing using a chemical-reactor-network model and found that 5–10 mol% additions of ethane or propane strongly promote methane ignition reducing delays by roughly 30–50%. Comparative studies on blended fuels, however, remain limited. While extensive data exist for pure fuels, fewer systematic studies consider binary blends under engine-relevant conditions. Lowry et al. [18] demonstrated synergistic effects in laminar flame speeds of methane/ethane/propane blends, emphasizing that blending can yield reactivity deviations that cannot be predicted by simple linear interpolation. Jach et al. [14] presented that fuel blending can influence ignition delay through changes in low-temperature radical and peroxide chemistry, for glycerol-doped gasoline and diesel surrogates over wide temperature and pressure ranges. Mixed reactors have also been used to study low-temperature oxidation and PAH production. Wang et al. [33] performed jet-stirred reactor experiments (600–1100 K, $\phi$ = 0.5–3.0) on acetylene, identifying aromatic intermediates including benzene, toluene, styrene and ethylbenzene, and establishing $C_2 + C_4 \rightarrow$ fulvene $\rightarrow$ benzene as the dominant low-temperature ring-formation route. Their accompanying mechanism (295 species) provided improved agreement for small hydrocarbons and early aromatics, though challenges remain for predicting larger PAHs. Similarly, Shao et al. [25] report high-pressure shock-tube ignition delay data for methane, ethylene, propene, and their binary blends using OH*, pressure, and IR absorption diagnostics, establish temperature-dependent scaling laws, and show strong synergistic effects, with certain $CH_4$/$C_2H_4$ mixtures igniting substantially faster than the pure fuels. At the mechanism-development level, multiple NUIG studies have compiled extensive databases of $C_1$–$C_2$ ignition delays. More recently, Baigmohammadi et al. [2] consolidated shock-tube and RCM IDTs for pure $CH_4$, $C_2H_4$ and $C_2H_6$ (800–2000 K, 1–80 bar), validating NUIGMech and mapping temperature-dependent sensitivities of $RO_2$, QOOH and $H_2O_2$ pathways. A follow-up study, Baigmohammadi et al. [1] extended the analysis to binary $C_1$-$C_2$ blends ($CH_4$/$C_2H_6$, $CH_4$/$C_2H_4$, $C_2H_4$/$C_2H_6$), providing improved NUIGMech1.0 validation, detailed sensitivity maps, and empirical ignition-delay correlations for engineering use within specified regimes. Martinez et al. [21] provide a comprehensive experimental and modelling dataset for $C_2$–$C_3$ binary blends across a broad range of temperatures (750–2000 K), pressures (1–135 bar), equivalence ratios and dilutions, and demonstrated that updated detailed kinetics in NUIGMech1.1 reveal strong synergistic effects of small propane additions at low temperatures. Cheng et al. [26] performed detailed shock-tube and rapid-compression-machine experiments on gasoline surrogates and ethanol blends, observing pronounced ethanol-induced suppression of low-temperature (NTC) reactivity and the disappearance of first-stage ignition at high ethanol levels, with modest promotion of reactivity at the highest temperatures. Additional mechanistic insight into additive effects comes from numerical reactor studies. The impact of $C_2$ additions on n-decane ignition was investigated by Huang et al. [13], who reported significant temperature-dependent effects: acetylene consistently increases ignition, ethylene promotes above 1000 K, and ethane inhibits below 1150 K but promotes at higher temperatures. Sensitivity analysis showed how tiny $C_2$ species may significantly change large-fuel ignition by identifying transitions between $H_2O_2$-dominated chain branching at low T and $HO_2$/OH/H-atom chemistry at higher T.

## 2. Experimental approach

The ignition delay studies were performed using the shock tube available at the Propulsion and High Enthalpy Lab, Karunya Institute of Technology and Sciences. Helium was used as the primary driver gas. To improve post-shock thermodynamic conditions, nitrogen is used as a tailoring gas. The stainless-steel shock tube has an internal diameter of 80 mm, with driver and driven section lengths of 2.0 m and 5.5 m respectively. Diaphragms were made of aluminium Al 6061, 1.2 mm thick, with a cross groove (0.5–0.6 mm) to enable measurements across a range of pressures (2–9 bar). Prior to each experiment, the test section and driven section were vacuumed to a pressure below $10^{-3}$ bar

using a turbo molecular pump to minimize the contamination effects on ignition delay measurements. Research-grade ethylene, acetylene, oxygen and nitrogen with purity ≥ 99.95% were used. When producing test gas mixtures, the fuel was first introduced into a thin-walled stainless-steel mixing tank at 8 bar using the partial pressure method. A three-test gas mixture was then prepared based on molar fractions using the partial pressure method. After filling, the mixtures were allowed to equilibrate for 30 minutes to ensure compositional homogeneity prior to experimentation. Table 1 displays the designed mixture composition for the experimental test. The shock tube facility used in this study has been extensively used in earlier investigations on ignition delay [22, 27–29], rupture dynamics [19, 30], and blast wave mitigation.

Table 1. Gas mixture compositions

| Mixture | Composition | $C_2H_4$ [%] | $C_2H_2$ [%] | Φ |
|---|---|---|---|---|
| 1 | $C_2H_4/C_2H_2/O_2/N_2$ | 95% | 5% | 1 |
| 2 | $C_2H_4/C_2H_2/O_2/N_2$ | 90% | 10% | 1 |
| 3 | $C_2H_4/C_2H_2/O_2/N_2$ | 80% | 20% | 1 |

Ignition delay time was determined using two diagnostics: (1) excited CH radical (CH*) emission near 431 nm, (ii) sidewall pressure measurements. The shock tube was physically cleaned with argon to reduce the effect of contaminants on the IDT results. Following this procedure, highly repeatable IDT data were obtained. Figure 1 shows the representative pressure and CH* chemiluminescence signals for three ethylene-acetylene/air mixtures at $\phi = 1.0$ from the oscilloscope.

## 3. Results and discussion

### 3.1. Ignition delay times for 95% ethylene/5%acetylene/ air mixtures

The reflected-shock temperature ($T_5$) and pressure ($P_5$) were computed from the measured incident-shock velocity using standard one-dimensional shock equations. Ignition delay was defined as the time interval between the arrival of the reflected shock and the maximum rate of rise of CH* chemiluminescence at 431 nm, a sensitive indicator of early hydrocarbon breakdown and radical formation. The CH* signal was detected using a photomultiplier with appropriate band-pass filtering. The repeatability of tests was verified through multiple tests at selected conditions, with an estimated overall uncertainty of ±10%, primarily due to uncertainties in temperature determination. Shock strength was adjusted by tailoring the driver gas composition, specifically the helium-to-nitrogen ratio. High-enthalpy conditions were achieved by increasing the helium partial pressure to 8 bar, resulting in higher incident shock velocities.

Ignition delay times for the $C_2H_4/C_2H_2$ (95/5) fuel-air mixture were measured behind reflected shocks over 580–1020 K and 2.7–8.4 bar. The experimental series covered a Mach number range of 1.67 to 2.45 for the reflected shock wave. Driver pressure ($P_4$) was varied between 6.4 and 9.3 bar, using different concentrations of Helium to obtain the shock strength. The post-reflected shock pressures ($P_5$) range from 2.7 bar to 8.4 bar. The data reveal the monotonic decrease in ignition delay with increasing temperature and pressure, represented by the following pressure-dependent Arrhenius correlation:

$$\tau = 4.58 \times 10^{-4} \exp(21930/RT_5)$$

Pearson correlation analysis confirms that temperature is the dominating parameter and $\ln(\tau)$ exhibits a strong negative correlation with $T_5$. Reflected-shock pressure also significantly influences reactivity. The ignition delay time for this mixture decreased monotonically as the reflected pressure and temperature increased (Fig. 2 and Fig. 3). The 95/5 mixture exhibited the longest ignition delay times

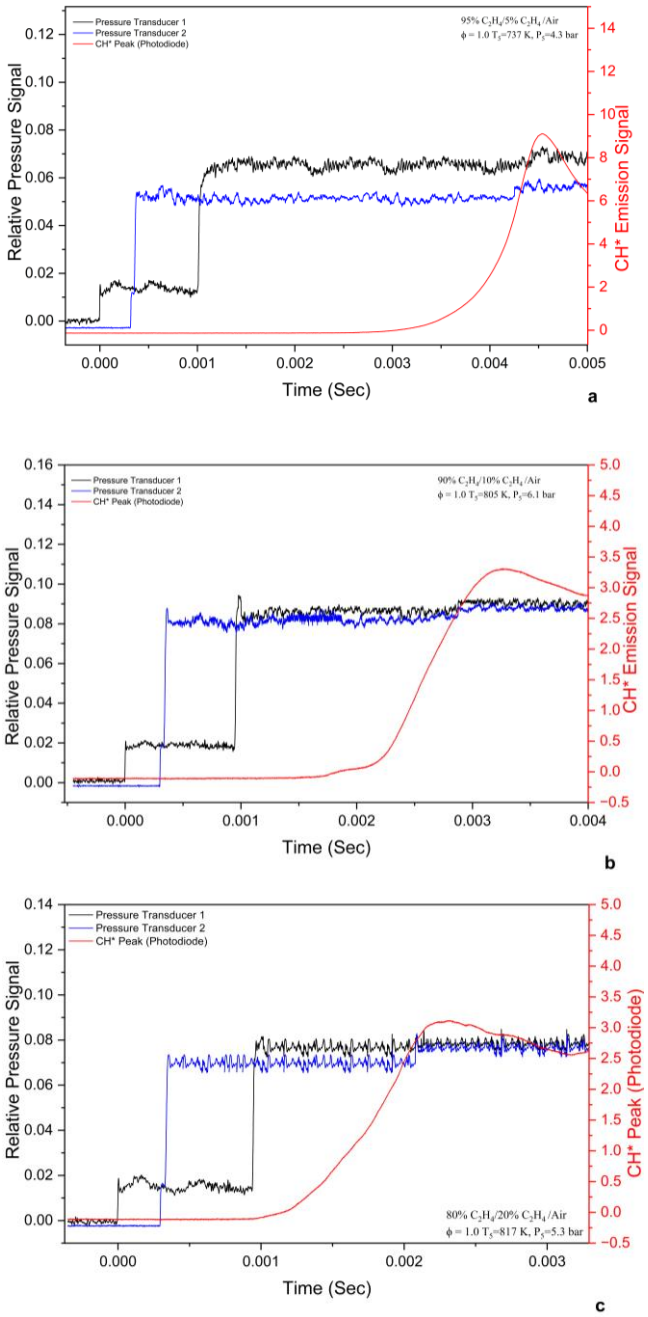


Fig. 1. Representative ignition delay time measurements for ethylene-acetylene/air mixtures at $\phi = 1.0$

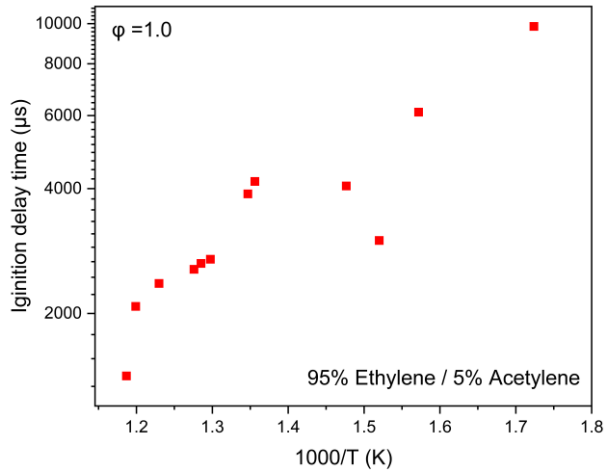


Fig. 2. Arrhenius plot for the ignition delay time of the 95% ethylene / 5% acetylene blend

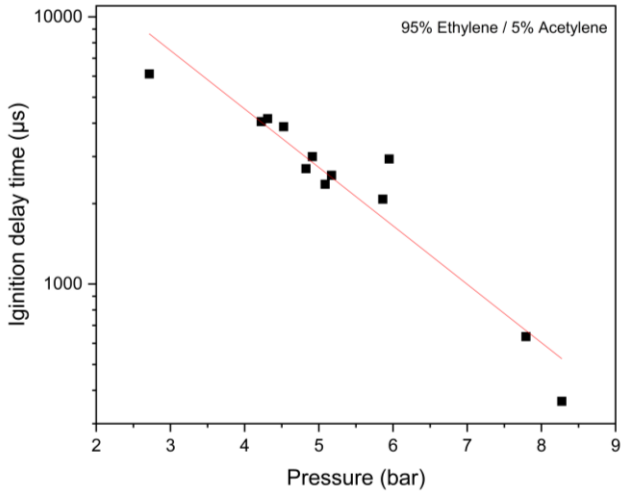


Fig. 3. Variation of ignition delay time with pressure for a 95% ethylene/ 5% acetylene mixture

among the three blends due to its lower oxidation pathways. At high pressure (7–8 bar), ignition delay time decreases, whereas at low pressure (3–4 bar) and temperature < 800 K, ignition delays exceed 6–10 ms.

### 3.2. Ignition delay times for 90% ethylene/ 10%acetylene/air mixtures

Ignition delay times were measured for a premixed ethylene/acetylene (90/10)-air mixture at an equivalence ratio of $\phi$ = 1.0 (Fig. 4 & 5) over a reflected-shock temperature range of 560 K to 1026 K. The incident shock Mach numbers range from 1.62 to 2.46, resulting in reflected shock pressures of 2.5-9.0 bar. The study exhibits strong Arrhenius behaviour, with IDT decreasing with increasing temperature. The shortest delay of 315 μs was observed at 1027 K, achieved using a helium-dominant driver gas. However, low-temperature study (560–650 K) highlights longer ignition delays exceeding 8ms, close to the limits of the shock tube's reliable test time. Strong negative statistical correlations indicate that an increase in driver helium fraction and shock strength consistently results in shorter ignition delays. The measured ignition delay times exhibited a strong inverse dependence on reflected shock temperature, consistent with Arrhenius kinetics. The experimental ignition delay times for the 90/10 ethylene-acetylene/air mixture were well represented by the following pressure-dependent Arrhenius correlation:

$$\tau = 2.54 \times 10^{-4} \exp(24430/RT_5)$$

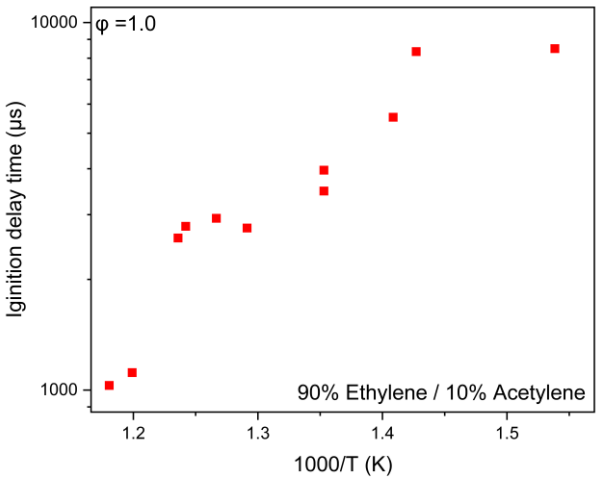


Fig. 4. Arrhenius plot for the ignition delay time of the 90% ethylene/10% acetylene blend

Influence diagnostics identify one low-temperature shot ($T_5$ = 560 K) as highly influential. Raw pressure and CH* traces for this data are inspected and found to be error-free. Hence, the point is retained in the global fit but noted as a possible exemplar of enhanced low-temperature variability.

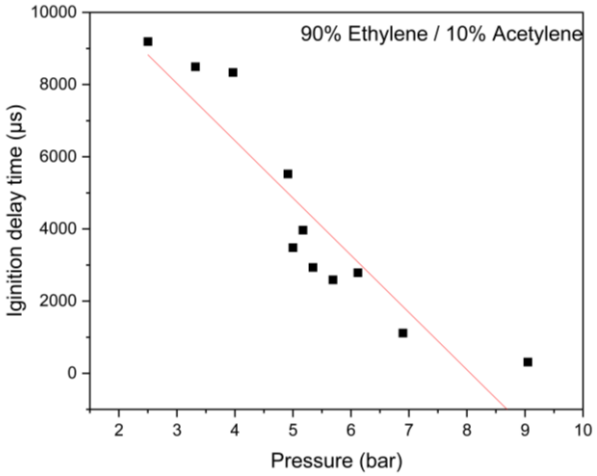


Fig. 5. Variation of ignition delay time with pressure for a 90% ethylene/ 10% acetylene mixture

The 90/10 mixture shows shorter ignition delays than the 95/5 blend, indicating the strong impact of increasing acetylene concentration. At a given pressure, ignition delays are about 40–60% shorter than in the 95/5 mixture.

### 3.3. Ignition delay times for 80% ethylene/ 20%acetylene/air mixtures

Ignition delay time measurements were obtained for a premixed 80% ethylene/20% acetylene-air mixture at an equivalence ratio of $\phi$ = 1.0 (Fig. 6 and Fig. 7). The post-

reflected-shock conditions spanned a temperature range of 650–870 K and pressures of 3.5–6.5 bar, covering the low to intermediate temperature ignition regime relevant to high-speed propulsion applications. The 80/20 mixture is the most reactive among the three blends and displays much shorter ignition delays.

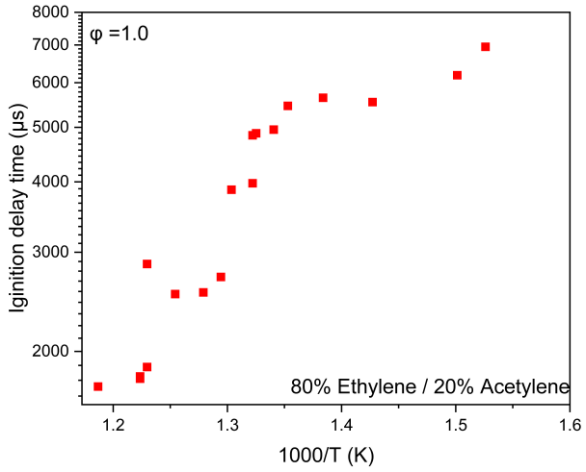


Fig. 6. Arrhenius plot for the ignition delay time of the 80% ethylene/20% acetylene blend

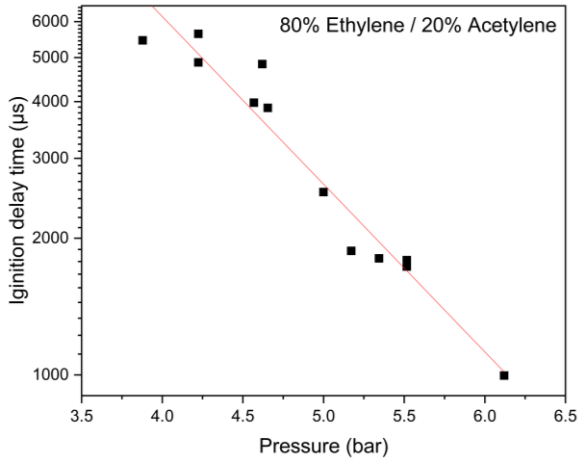


Fig. 7. Variation of ignition delay time with pressure for 80% ethylene/ 20% acetylene mixture

The measured ignition delays exhibit a strong Arrhenius-type temperature dependence. The statistical correlations demonstrate that driver composition and shock strength parameters strongly influence ignition delay. Increased helium fraction, higher shock velocity, and higher shock Mach number all correlate with progressively shorter ignition delays. These factors increase incident-shock strength and raise the reflected-shock temperature, thereby accelerating the production of H, O, and OH radicals. At low temperatures (650–700 K), longer ignition delays up to 7 ms were observed, indicating slow radical buildup dominated by peroxy and $HO_2$ chemistry. In the intermediate range (720–790 K), the measured data show a rapid decrease in delay time, consistent with the onset of high-temperature chain-branching reactions. At higher temperatures (> 800 K), ignition occurs rapidly (< 2 ms) due to accelerated decomposition pathways in acetylene and ethylene. Repeatability was confirmed at intermediate temperatures, specifically, three independent shocks near 815 K yielded highly consistent IDTs clustered around 1800 ±50 μs.

A mild pressure dependence was observed, with τ decreasing approximately as $P^{-0.6}$. The experimental data were fitted using a modified Arrhenius correlation of the form:

$$\tau = 7.1 \times 10^{-5} \exp(40300/RT_5)$$

The fitted correlation aligns well with the experimental ignition delay time between 650–870 K and 4–6 bar. With $R^2 = 0.808$, the model captures nearly 81% of the variance in ln(τ) based on temperature and pressure dependencies. The RMSE in ln-space was 0.219, which corresponds to a multiplicative 1σ uncertainty factor of 1.24, or roughly ±24% deviation between measured and predicted ignition delay times. This level of scatter is consistent with reflected-shock ignition measurements at low and intermediate temperatures, where small uncertainties in $T_5$ (±5–10 K) produce large exponential variations in ignition delay.

### 3.4. Comparative effect of acetylene addition on ignition delay

Comparison of ignition delay times for the three ethylene-acetylene/air blends investigated in this study (Fig. 8). IDT measurements for acetylene [27] and ethylene [15] were performed using the same facility (Table 2). Under similar temperature and pressure conditions, increasing acetylene fraction results in a monotonic reduction in ignition delay time. Approximately at 800 K and 4 bar, the 90/10 blend ignites 40–50% faster than the 95/5 mixture, while the 80/20 blend exhibits a further reduction of 20–30%.

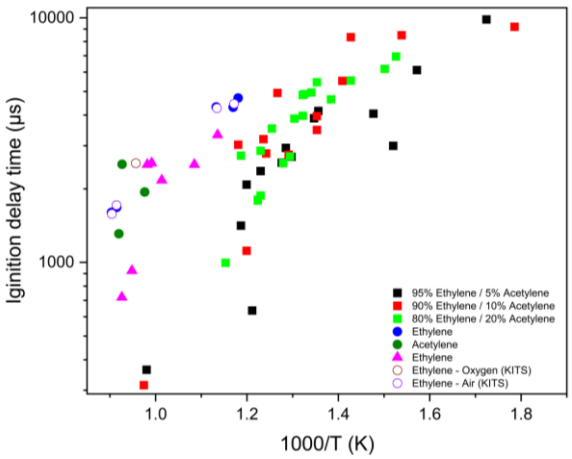


Fig. 8. Arrhenius plot comparing ignition delay times for various ethylene/ acetylene fuel blends and pure components

Table 2. Ignition delay trends for ethylene- acetylene blends

| Blend | Relative IDT | Pressure sensitivity | Dominant chemistry |
|---|---|---|---|
| 95/5 | Longest | Strong | $HO_2$–$H_2O_2$ dominated |
| 90/10 | Intermediate | Moderate | Mixed $HO_2$/HCCO |
| 80/20 | Shortest | Weak | HCCO-driven OH |

## 4. Kinetic modelling

In this work, CHEMKIN simulations were carried out using four mechanisms – NUIG [34], ARAMCO [35], LLNL [20], and SD [5] to evaluate autoignition of three mixtures. IDT is defined numerically as the maximum gradient of temperature and OH/CH radical concentration with respect to time for the shock tube simulations. All mechanisms failed to predict ignition below 750 K, indicating the absence of low-temperature peroxy and QOOH pathways that are essential for $C_2$ hydrocarbon oxidation. In the temperature region (900–1100 K), the NUIG and ARAMCO mechanisms produced physically reasonable ignition delay trends, with NUIG showing the closest agreement to experimental timescales and Arrhenius behaviour. In contrast, the LLNL and SD mechanisms displayed non-physical trends, including excessively long delays and increased ignition times at higher temperatures. Among the mechanisms considered, NUIG exhibits the highest computational cost, followed by Aramco, LLNL and San Diego mechanism. This is mainly due to differences in the number of species, reactions, and pressure-dependent formulations included in each mechanism. Across all four mechanisms, increasing acetylene content systematically reduces the ignition delay.

### 4.1. Ignition kinetics of ethylene-acetylene blends using the ARAMCO mechanism

Sensitivity analysis (Fig. 9) identifies $H_2O_2(+M) \rightleftharpoons 2OH(+M)$ as the key promoting reaction for ignition across all three blends, controlling the transition from $HO_2$-dominated induction phase to rapid OH-driven chain branching. The sensitivity of this reaction increases with acetylene fraction, and reaches a maximum for the 80% ethylene-20% acetylene mixture, indicating a stronger dependence of ignition on peroxide decomposition in acetylene-rich blends. Additionally, $C_2H_4 + HO_2 \rightleftharpoons C_2H_4O + OH$ and $C_2H_3 + O_2 \rightleftharpoons CH_2CHO + O$, directly contribute to OH and atomic oxygen formation, reflecting enhanced coupling between ethylene oxidation and acetylene-derived radical pathways.

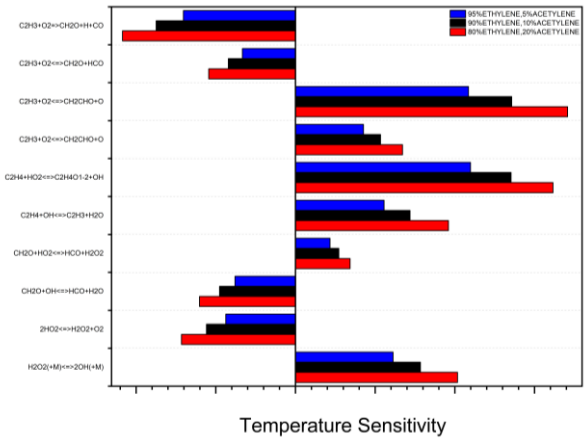


Fig. 9. Temperature sensitivity analysis (Aramco mechanism)

The dominant inhibiting reactions (Fig. 9) include $2HO_2 \rightleftharpoons H_2O_2 + O_2$, $CH_2O + OH \rightleftharpoons HCO + H_2O$, and $C_2H_3 + O_2 \rightarrow CH_2O + HCO$, which suppress ignition by recombining radicals into less reactive reservoirs. Although these inhibiting pathways remain significant for all mixtures, their influence decreases with increasing acetylene content, indicating that acetylene-derived radical chemistry compensates for radical losses. Table 3 summarises the dominant reactions for 95% $C_2H_4$ / 5% $C_2H_2$ (Aramco).

Table 3. Top sensitivity reactions – Aramco mechanism (95% $C_2H_4$/5% $C_2H_2$)

| Rank | Reaction | Sensitivity | Effect |
|---|---|---|---|
| 1 | $C_2H_4 + HO_2 \rightleftharpoons C_2H_4O + OH$ | 2198 | Accelerates ignition |
| 2 | $C_2H_3 + O_2 \rightleftharpoons CH_2CHO + O$ | 2171 | Accelerates ignition |
| 3 | $H_2O_2 (+M) \rightleftharpoons 2OH (+M)$ | 1225 | Accelerates ignition |
| 4 | $C_2H_3 + O_2 \rightleftharpoons CH_2O + HCO$ | -667 | Inhibits ignition |
| 5 | $CH_2O + OH \rightleftharpoons HCO + H_2O$ | -760 | Inhibits ignition |

ROP analysis at 850 K and 2 bar (Fig. 10–12) reveals that OH formation is dominated by $O_2 + H \rightleftharpoons O + OH$, followed by $O + H_2O \rightleftharpoons 2OH$ and $HO_2 + H \rightleftharpoons 2OH$. The contribution of these reactions increases with the acetylene fraction, particularly for $O_2 + H \rightleftharpoons O + OH$, indicating greater availability of atomic hydrogen. This enhancement arises from acetylene oxidation pathways involving HCCO and $CH_2CO$ chemistry, leading to earlier radical runaway in acetylene mixtures. The dominant OH absorption reactions include $CO + OH \rightleftharpoons CO_2 + H_2$, $CH_2O + OH \rightleftharpoons HCO + H_2O$, and $HCCO + OH \rightarrow H_2 + 2CO$, with the importance of HCCO related OH consumption increasing as acetylene fraction raises. HCCO formation is dominated by $C_2H_2 + O \rightleftharpoons HCCO + H$, with secondary contribution from $CH_2CO + H \rightleftharpoons HCCO + H_2$ and $CH_2CO + OH \rightleftharpoons HCCO + H_2O$, confirming acetylene as primary driver of $C_2$ radical chemistry. HCCO consumption occurs mainly through reactions with OH, O, and H, which regenerate H and O atoms, and directly reinforce OH formation pathways. The $H_2O_2$ ROP study confirms that peroxide chemistry acts as the primary ignition bottleneck, $H_2O_2$ accumulates primarily through $HO_2$ recombination and subsequently decomposes through

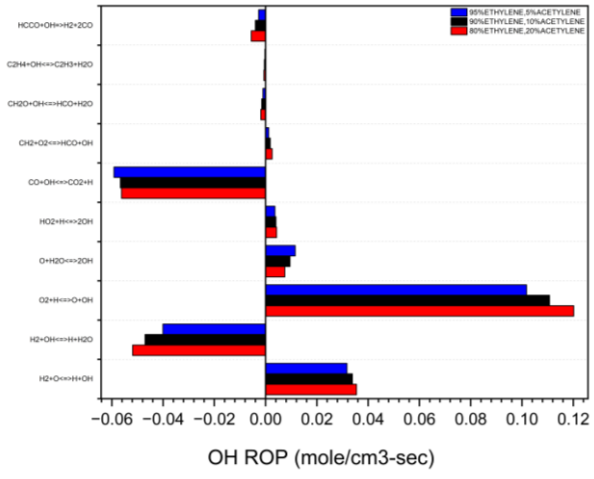


Fig. 10. Rate of production analysis of OH (Aramco mechanism)

$H_2O_2(+M) \rightleftharpoons 2OH(+M)$, triggering rapid OH release. Increasing acetylene fraction, enhances the net decomposition rate of $H_2O_2$, thereby accelerating the transition from $HO_2$ controlled chemistry to OH dominated chain branching.

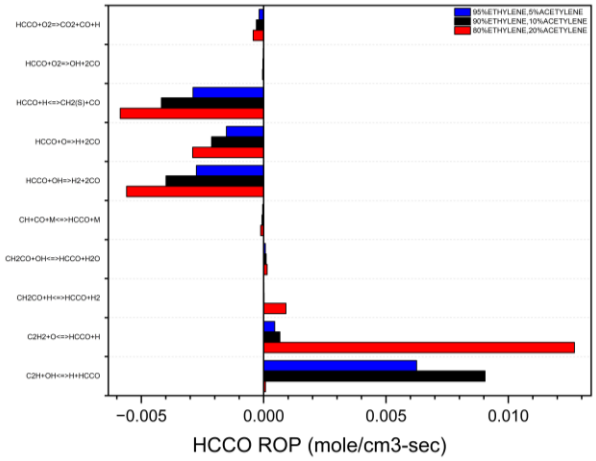


Fig. 11. Rate of production analysis of HCCO (Aramco mechanism)

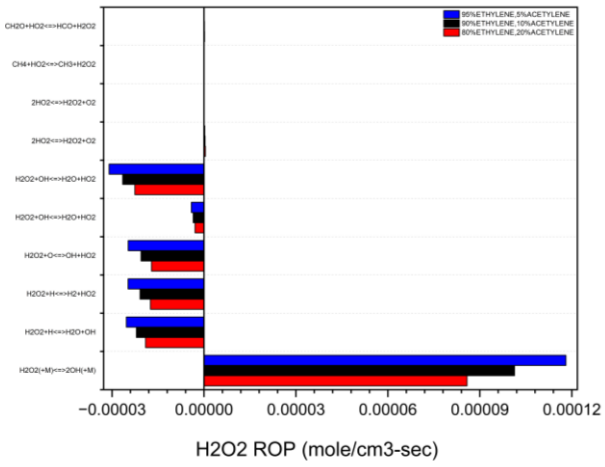


Fig. 12. Rate of production analysis of $H_2O_2$ (Aramco mechanism)

### 4.2. Ignition kinetics of ethylene–acetylene blends using the LLNL mechanism

The sensitivity study using the LLNL mechanism at 850 K and 2 bar presented (Fig. 13) reveals that ignition of ethylene-acetylene mixtures is predominantly governed by peroxide-driven radical branching. Across all three blends, the most influential ignition-promoting reaction is $2OH (+M) \rightleftharpoons H_2O_2 (+M)$, confirming that ignition onset is controlled by transition from a peroxide-dominated radical reservoir to rapid OH chain branching. In addition, acetylene oxidation exhibits strong positive sensitivity, particularly $C_2H_2 + O_2 \rightleftharpoons HCCO + OH$, demonstrating that LLNL mechanism strongly couples acetylene consumption to OH formation, partially bypassing slower $HO_2$ mediated pathways. The sensitivity decreases with decreasing acetylene fraction but remains significant even at 5% acetylene. Ethylene abstraction reactions such as $C_2H_4 + OH \rightleftharpoons C_2H_3 + H_2O$ also promote ignition by accelerating fuel breakdown and radical propagation. The dominant inhibiting reactions (Fig. 17), includes $C_2H_3 + O_2 \rightleftharpoons CH_2O + HCO$, $CH_2O + OH \rightleftharpoons HCO + H_2O$, and $H_2O_2 + OH \rightleftharpoons H_2O + HO_2$, suppress ignition by redirecting reactive radicals into less active reservoirs. Table 4 summarises the dominant reactions identified in sensitivity analysis for 80% $C_2H_4$/20% $C_2H_2$ (LLNL)

Table 4. Top sensitivity reactions – LLNL mechanism (80% $C_2H_4$/20% $C_2H_2$)

| Rank | Reaction | Sensitivity | Effect |
|---|---|---|---|
| 1 | $C_2H_2 + O_2 \rightleftharpoons HCCO + OH$ | 7166 | Accelerates ignition |
| 2 | $2OH (+M) \rightleftharpoons H_2O_2 (+M)$ | 5126 | Accelerates ignition |
| 3 | $C_2H_3 + O_2 \rightleftharpoons CH_2HCO + O$ | 3813 | Accelerates ignition |
| 4 | $C_2H_3 + O_2 \rightleftharpoons CH_2O + HCO$ | –3723 | Inhibits ignition |
| 5 | $C_2H_4 + OH \rightleftharpoons C_2H_3 + H_2O$ | 2256 | Accelerates ignition |

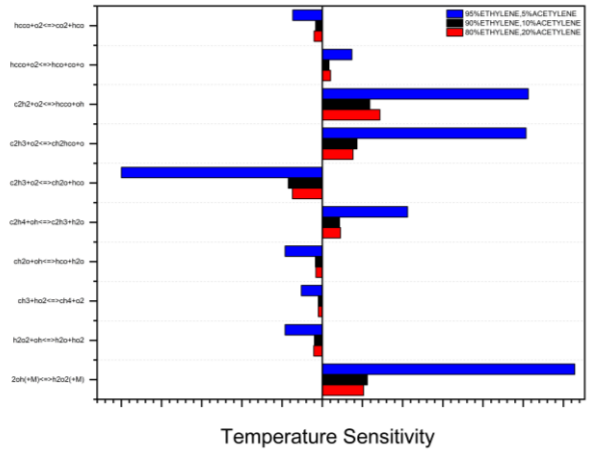


Fig. 13. Temperature sensitivity analysis (LLNL mechanism)

The OH ROP analysis (Fig. 14) indicates that OH production in the LLNL mechanism is dominated by H-O interconversion reactions once sufficient atomic oxygen is available, with $O + H_2 \rightleftharpoons OH + H$ and $O + OH \rightleftharpoons O_2 + H$. dominating during the rapid ignition phase. $HO_2$ chemistry indirectly serves primarily as a precursor to H2O2, which subsequently decomposes, triggering OH runaway. Increasing the acetylene fraction moderately enhances OH production by increasing the availability of H and O atoms. However, peroxide decomposition remains the principal ignition trigger across all blends.

HCCO (Fig. 15) emerges as a key intermediate in the LLNL mechanism linking to radical regeneration. HCCO formation is dominated by $C_2H_2 + O \rightleftharpoons HCCO + H$, with secondary contributions from $CH_2CO$ based pathways. HCCO consumption occurs primarily through reactions with H, O, and OH, all of which regenerate H and O atoms, thereby yielding OH.

The $H_2O_2$ ROP analysis (Fig. 16) confirms that peroxide chemistry acts as the rate-limiting ignition bottleneck in the LLNL mechanism. During the induction period, $H_2O_2$ is

slowly formed by $HO_2$ recombination and decomposes rapidly near ignition, releasing OH and initiating chain branching. Although acetylene addition slightly accelerates decomposition by increasing radical availability, peroxide breakdown remains the controlling step for ignition across all mixtures.

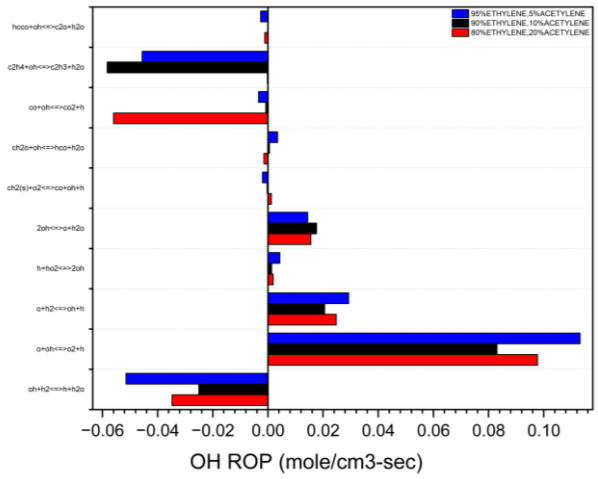


Fig. 14. Rate of production analysis of OH (LLNL mechanism)

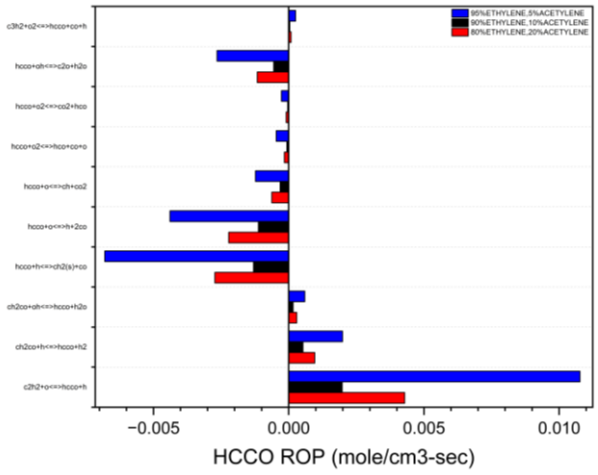


Fig. 15. Rate of production analysis of HCCO (LLNL mechanism)

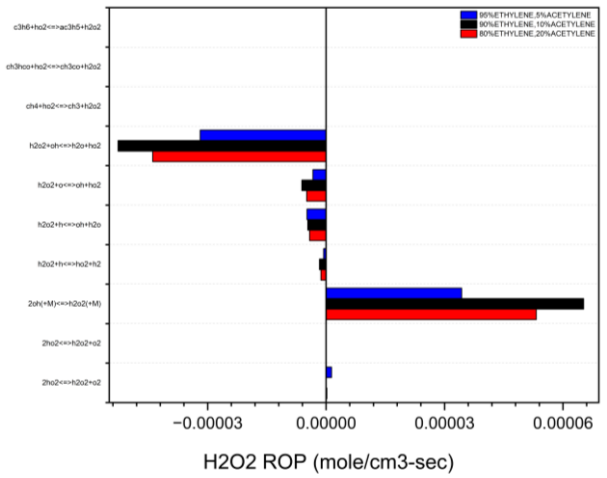


Fig. 16. Rate of production analysis of $H_2O_2$ (LLNL mechanism)

### 4.3. Ignition kinetics of ethylene–acetylene blends using SD mechanism

The sensitivity study using the SD mechanism at 850 K and 2 bar (Fig. 17) shows that the ignition of ethylene–acetylene blends is primarily governed by peroxide-controlled chemistry. The dominant reaction across all mixtures is $2OH\ (+M) \rightleftharpoons H_2O_2\ (+M)$, indicating that ignition onset is dictated by the transition from $HO_2/H_2O_2$ dominated chemistry to rapid OH radical chain branching.

This sensitivity increases with acetylene fraction and is highest for the 90/10 and 80/20 mixtures, highlighting the significance of peroxide-controlled ignition pathways. Furthermore, promoting reactions include $C_2H_4 + HO_2 \rightleftharpoons C_2H_4O + OH$ and $C_2H_2 + OH \rightleftharpoons C_2H_3 + H_2O$, highlighting the role of fuel-assisted conversion in accelerating ignition (Table 5). In contrast, reactions such as $2HO_2 \rightleftharpoons H_2O_2 + O_2$ and $CH_2O + OH \rightleftharpoons HCO + H_2O$ retard ignition by limiting OH buildup.

Table 5. Top sensitivity reactions – SD mechanism (90% $C_2H_4$/10% $C_2H_2$)

| Rank | Reaction | Sensitivity | Effect |
|---|---|---|---|
| 1 | $C_2H_3 + O_2 \rightleftharpoons CH_2CHO + O$ | 16695 | Accelerates ignition |
| 2 | $C_2H_3 + O_2 \rightleftharpoons CH_2O + HCO$ | –14180 | Inhibits ignition |
| 3 | $C_2H_4 + HO_2 \rightleftharpoons C_2H_4O + OH$ | 9935 | Accelerates ignition |
| 4 | $2OH\ (+M) \rightleftharpoons H_2O_2\ (+M)$ | 8037 | Accelerates ignition |
| 5 | $CH_2O + OH \rightleftharpoons HCO + H_2O$ | –1900 | Inhibits ignition |

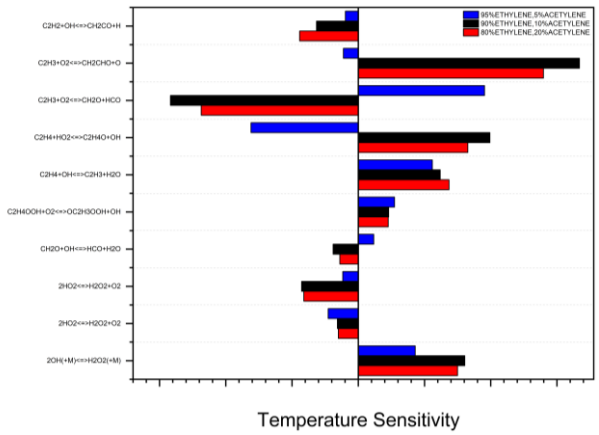


Fig. 17. Temperature sensitivity analysis (SD mechanism)

ROP analysis (Fig. 18–20), reveals that OH formation in the SD mechanism is dominated by classical H-O chain-branching reactions, with $H + O_2 \rightleftharpoons OH + O$ as principal source of OH once ignition is initiated. Increasing acetylene fraction enhances the contribution of these reactions by increasing the availability of H and O atoms through $C_2$ chemistry. OH consumption pathway is dominated by $CO + OH \rightleftharpoons CO_2 + H$, $CH_2O + OH \rightleftharpoons HCO + H_2O$, and $CH_3 + OH \rightleftharpoons CH_2 + H_2O$, which act as strong sinks during the induction period.

The HCCO formation (Fig. 19) is dominated by $C_2H_2 + O \rightleftharpoons HCCO + H$, with additional contributions from ketene related pathways. The monotonic increase in HCCO for-

mation with acetylene fraction confirms that acetylene directly enhances $C_2$ radical chemistry. HCCO consumption occurs primarily through H, O and $O_2$, regenerating reactive radicals and contributing to chain branching. Despite this enhancement, the $H_2O_2$ ROP analysis (Fig. 20) reveals that peroxide decomposition remains the dominant ignition bottleneck in the SD mechanism, with acetylene addition moderately accelerating the transition to OH-dominated chemistry.

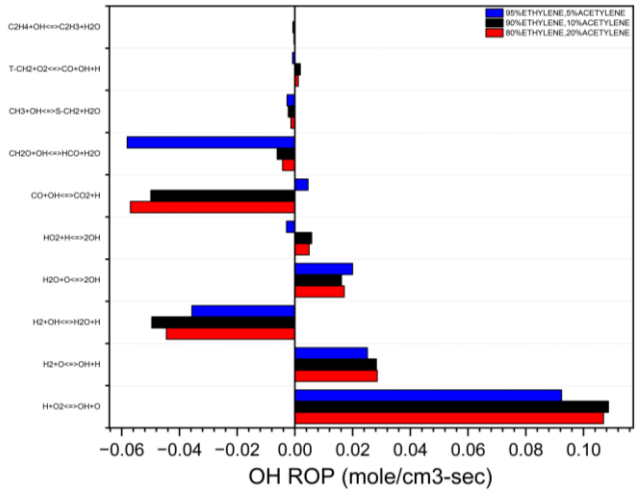


Fig. 18. Rate of production analysis of OH (SD mechanism)

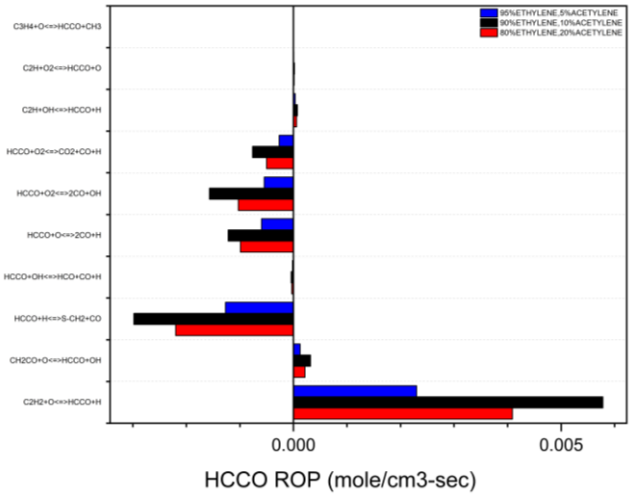


Fig. 19. Rate of production analysis of HCCO (SD mechanism)

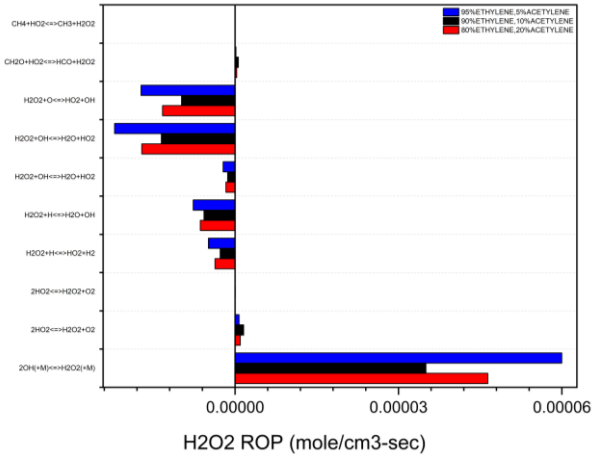


Fig. 20. Rate of production analysis of $H_2O_2$ (SD mechanism)

## 5. Conclusion

Ignition delay characteristics of binary ethylene–acetylene/air mixtures were experimentally investigated in a shock tube over 560–1030 K and 2.5–9 bar at $\phi$ = 1.0 for three blend ratios. The ignition delay time decreases with increasing acetylene fraction, with reductions up to ~60% for an 80% $C_2H_4$–20% $C_2H_2$ mixture relative to a 95% $C_2H_4$–5% $C_2H_2$ mixture at comparable temperature – pressure conditions. Among the tested blends, the 80% ethylene–20% acetylene mixture exhibits the shortest ignition delays and the earliest onset of OH radical emission, while the 95% ethylene 5% acetylene mixture displays the longest induction periods and the greatest pressure sensitivity. Arrhenius correlations confirm that temperature remains the dominant controlling parameter, with acetylene addition gradually shifting toward faster ignition.

The systematic underprediction of ignition reactivity by all kinetic mechanisms (NUIG, ARAMCO, LLNL, and San Diego) below 750 K highlights persistent deficiencies in low-temperature $C_2$ oxidation chemistry and in cross-fuel radical coupling. Across all mechanisms, ignition is controlled by $HO_2$–$H_2O_2$ chemistry, with thermal decomposition of $H_2O_2$ acting as the primary trigger for OH radical runaway. Acetylene enhances ignition by strengthening HCCO-mediated radical-regeneration pathways, increasing H and O atom availability, and accelerating the transition from peroxide-controlled induction to chain-branching chemistry. These findings demonstrate that acetylene addition can significantly enhance ethylene ignition under short-residence-time conditions, providing direct guidance for fuel formulation and kinetic model development for scramjet and high-speed propulsion systems.

## Nomenclature

| | |
|---|---|
| A | pre-exponential factor |
| $C_2H_4$ | ethylene |
| $C_2H_2$ | acetylene |
| $CH_2O$ | formaldehyde |
| CH* | chemiluminescence of the excited CH radical |
| $E_a$ | apparent activation energy |
| HCO | formyl radical |
| $HO_2$ | hydroperoxyl radical |
| $H_2O_2$ | hydrogen peroxide |
| HCCO | ketyl radical |
| OH | hydroxyl radical |
| IDT | ignition delay time |
| LLNL | Lawrence Livermore National Laboratory mechanism |

| | | | |
|---|---|---|---|
| NUIG | National University of Ireland, Galway mechanism | SD | San Diego mechanism |
| ROP | rate of production | $\tau$ | ignition delay time |

## Bibliography


[1] Baigmohammadi M, Patel V, Nagaraja S, Ramalingam A, Martinez S, Panigrahy S. Comprehensive experimental and simulation study of the ignition delay time characteristics of binary blended methane, ethane, and ethylene over a wide range of temperature, pressure, equivalence ratio, and dilution. Energy Fuels. 2020;34(7):8808-8823. https://doi.org/10.1021/acs.energyfuels.0c00960

[2] Baigmohammadi M, Patel V, Martinez S, Panigrahy S, Ramalingam A, Burke U. A comprehensive experimental and simulation study of ignition delay time characteristics of single fuel C1-C2 hydrocarbons over a wide range of temperatures, pressures, equivalence ratios, and dilutions. Energy Fuels. 2020;34(3):3755-3771. https://doi.org/10.1021/acs.energyfuels.9b04139

[3] Boruc ŁJ, Kapusta J, Kindracki J. Selection of the method for determination of ignition delay of hypergolic propellants. Combustion Engines. 2024;199(4):104-111. https://doi.org/10.19206/CE-192420

[4] Burcat A, Scheller K, Lifshitz A. Shock-tube investigation of comparative ignition delay times for C1-C5 alkanes. Combust Flame. 1971;16(1):29-33. https://doi.org/10.1016/S0010-2180(71)80007-X

[5] Chemical-kinetic mechanisms for combustion applications. San Diego Mechanism Web Page. University of California San Diego. Available from: http://combustion.ucsd.edu

[6] Dagaut P, Boettner JC, Cathonnet M. Ethylene pyrolysis and oxidation: A kinetic modeling study. Int J Chem Kinet. 1990;22(6):641-664. https://doi.org/10.1002/kin.550220608

[7] Dagaut P, Cathonnet M, Boettner J. Kinetics of ethane oxidation. Int J Chem Kinet. 1991;23(5):437-455. https://doi.org/10.1002/kin.550230509

[8] De Vries J, Hall JM, Simmons SL, Rickard MJA, Kalitan DM. Ethane ignition and oxidation behind reflected shock waves. Combust Flame. 2007;150:137-150. https://doi.org/10.1016/j.combustflame.2006.10.008

[9] De Vries J, Petersen EL. Autoignition of methane-based fuel blends under gas turbine conditions. Proc Combust Inst. 2007;31(2):3163-3171. https://doi.org/10.1016/j.proci.2006.07.206

[10] Gallagher SM, Curran HJ, Metcalfe WK, Healy D, Simmie JM, Bourque G. Rapid compression machine study of propane oxidation in the negative temperature coefficient regime. Combust Flame. 2008;153(1-2):316-333. https://doi.org/10.1016/j.combustflame.2007.09.004

[11] Herzler J, Jerig L, Roth P. Shock-tube study of the ignition of propane at intermediate temperatures and high pressures. Combust Sci Technol. 2004;176(10):1627-1637. https://doi.org/10.1080/00102200490487201

[12] Holton M, Gokulakrishnan P, Klassen MS, Roby RJ, Jackson GS. Autoignition delay time measurements of methane, ethane, and propane pure fuels and methane-based fuel blends. J Eng Gas Turbines Power. 2010;132(9):1-9. https://doi.org/10.1115/1.4000590

[13] Huang J, Li F, Qi Y. Comparative study on the impact of ethane/ethylene/acetylene addition on ignition of fuel-rich n-decane/air flame. Bull Ser B. 2020;82(4):185-198.

[14] Jach I, Cieślak I, Teodorczyk A. Investigation of glycerol doping on ignition delay times and laminar burning velocities of gasoline and diesel fuel. Combustion Engines. 2017;169(2):167-175. https://doi.org/10.19206/ce-2017-230

[15] Kesavan M, Sundararaj AJ, Williams M, Konda S, Kumar W. Experimental investigation of auto ignition of ethylene and propulsion grade kerosene. Russ J Phys Chem B. 2025; 19(6):1338-1352. https://doi.org/10.1134/S1990793125701076

[16] Kopp M, Donato NS, Petersen EL, Metcalfe WK, Burke SM, Curran HJ. Oxidation of ethylene-air mixtures at elevated pressures, part 1: experimental results. J Propuls Power. 2014;30(3):790-798. https://doi.org/10.2514/1.B34890

[17] Leschevich VV, Martynenko VV, Penyazkov OG, Sevrouk KL, Shabunya SI. Auto-ignitions of a methane/air mixture at high and intermediate temperatures. Shock Waves. 2016; 26(5):657-672. https://doi.org/10.1007/s00193-016-0665-9

[18] Lowry W, De Vries J, Krejci M, Petersen E, Serinyel Z, Metcalfe W. Laminar flame speed measurements and modeling of pure alkanes and alkane blends at elevated pressures. J Eng Gas Turbines Power. 2011;133(9):1-9. https://doi.org/10.1115/1.4002809

[19] Lyle JL, Guna KR, Kumar P, Sundararaj AJ. Rupture dynamics of shock-tube diaphragm. Proc Int Conf Recent Adv Aerosp Eng (ICRAAE). 2017:1-4. https://doi.org/10.1109/ICRAAE.2017.8297207

[20] Marinov NM, Pitz WJ, Westbrook CK, Vincitore AM, Castaldi MJ. Aromatic and polycyclic aromatic hydrocarbon formation in a laminar premixed n-butane flame. Combust Flame. 1998;114(1-2):192-213. https://doi.org/10.1016/S0010-2180(97)00275-7

[21] Martinez S, Patel V, Panigrahy S, Sahu A, Nagaraja B. Experimental and kinetic modeling study of ignition delay characteristics of ethane/propane and ethylene/propane blends. Combust Flame. 2021;228:401-414. https://doi.org/10.1016/j.combustflame.2021.02.009

[22] Rose MS, Sundararaj AJ, Kumar S. Investigation of ignition delay of hydrocarbon fuel using shock tube. Int J Pure Appl Math. 2018;118(20):3687-3692.

[23] Sander R, Longwic R, Tarkowski S. Analysis of the influence of the n-hexane content in the mixture with rapeseed oil on the auto-ignition delay angle of the fuel. Combustion Engines. https://doi.org/10.19206/CE-211729

[24] Saxena S, Kahandawala MSP. Shock tube study of ignition delay in the combustion of ethylene. Combust Flame. 2011;158(6):1019-1031. https://doi.org/10.1016/j.combustflame.2010.10.011

[25] Shao J, Davidson DF. Shock tube study of ignition delay times in diluted methane, ethylene, propene and their blends at elevated pressures. Fuel. 2018;225:370-380. https://doi.org/10.1016/j.fuel.2018.03.146

[26] Song C, Saggese C, Kang D, Goldsborough SS, Wagnon SW, Kukkadapu G. Autoignition and heat release of gasoline surrogates and ethanol blends at engine-relevant conditions. Combust Flame. 2021;228:57-77. https://doi.org/10.1016/j.combustflame.2021.01.033

[27] Sundararaj AJ, Pillai BC, Subash AN, Haran AP, Kumar P. Investigation of ignition delay for low molecular weight hydrocarbon fuel using shock tube in reflected shock mode. J Geol Soc India. 2019;93:218-220. https://doi.org/10.1007/s12594-019-1155-3

[28] Sundararaj AJ, Pillai BC, Guna KR. Effect of temperature on ignition behaviour of seeded refined kerosene. Thermochim Acta. 2020;683:178469. https://doi.org/10.1016/j.tca.2019.178469
[29] Sundararaj AJ, Guna KR, William M. Effect of temperature on ignition of modified kerosene. Int J Engine Res. 2022; 23(3):460-468. https://doi.org/10.1177/1468087420988191
[30] Sundararaj AJ, Jose D, Sunny A, John ST, Kumar N, Gopalsamy. Effect of blast pressure on discrete models using a shock tube. Proc Int Conf Recent Adv Aerosp Eng (ICRAAE). 2017:1-4. https://doi.org/10.1109/ICRAAE.2017.8297238
[31] Walker BC. Shock-tube investigation of ignition delay times of blends of methane and ethane with oxygen. Aerosp Eng Commons. 2007. https://stars.library.ucf.edu/etd/3399/
[32] Wan Z, Zheng Z, Wang Y, Zhang D, Li P, Zhang C. Shock tube study of ethylene/air ignition characteristics over a wide temperature range. Combust Sci Technol. 2020; 192(12):2297-2305. https://doi.org/10.1080/00102202.2019.1643333
[33] Wang H, Liu Y, Weng J, Glarborg P, Tian Z. New insights in low-temperature oxidation of acetylene. Proc Combust Inst. 2017;36(1):355-363. https://doi.org/10.1016/j.proci.2016.06.163
[34] Wang H, Dames E, Sirjean B, Sheen DA, Tango R, Violi A. High-temperature chemical kinetic model of n-alkanes and cycloalkanes oxidation (JetSurF). Available from: http://web.stanford.edu/group/haiwanglab/JetSurF/
[35] Zhou CW, Li Y, Burke U, Banyon C, Somers KP. Experimental and kinetic modeling study of 1,3-butadiene combustion: ignition delay time and laminar flame speed measurements. Combust Flame. 2018;197:423-438. https://doi.org/10.1016/j.combustflame.2018.08.006

Kesavan Marimuthu – Division of Aerospace Engineering, Karunya Institute of Technology and Sciences, India.
e-mail: *m.kesavan02@gmail.com*

Aldin Justin Sundararaj – Division of Aerospace Engineering, Karunya Institute of Technology and Sciences, India.
e-mail: *aldinjustin@karunya.edu*

Abhijith Girish Nair – Division of Aerospace Engineering, Karunya Institute of Technology and Sciences, India.
e-mail: *abhijithg.n963@gmail.com*

Thangapandi Muthumari – Division of Aerospace Engineering, Karunya Institute of Technology and Sciences, India.
e-mail: *t.muthumarikesavan@gmail.com*